Resveratrol slows down epithelial-mesenchymal transition in hepatocellular carcinoma via modulation of Akt/GSK3β/SNAIL1 signaling pathway

Section A -Research paper

RESVERATROL SLOWS DOWN EPITHELIAL-MESENCHYMAL TRANSITION IN HEPATOCELLULAR CARCINOMA VIA MODULATION OF AKT/GSK3B/SNAIL1 SIGNALING PATHWAY

Asmaa M.A. Bayoumi[1], Esraa M.M.A. Khalifa[2], Mohamed M. Sayed-Ahmed[3], Marwa Sharaky[4], Maiiada H. Nazmy[1]*

ABSTRACT

Background: Epithelial-mesenchymal transition (EMT) is one of the main targets for controlling hepatocellular carcinoma (HCC). In this study, resveratrol (RES) was evaluated for its anti-cancer activity *in vivo* via modulation of EMT in HCC, and for its pro-apoptotic activity in HepG2 cell line *in vitro*. **Methods:** Rats were divided into five groups. Group-1 received the vehicles; Group-2 received RES; Group-3 received diethylnitrosamine (DEN) and carbon tetrachloride (CCl_4); Group-4 received RES pretreatment and DEN/CCl_4; Group-5 received DEN/CCl_4 and RES posttreatment. Oxidative stress and hepatic function were evaluated. Akt and glycogen synthesis kinase-3β (GSK3β) expression levels were determined. Furthermore, the impact of RES on HepG2 cell viability was investigated. **Results:** RES provided hepatoprotective effects, which were verified by biochemical and histopathological findings. EMT markers were modulated by RES. It reduced the expression of TGF-β1 and SNAIL1 and increased that of E-cadherin protein. RES led to up-regulation of GSK3β and down-regulation of Akt. HepG2 cells viability was reduced by RES, causing apoptosis and arresting HepG2 cells in the G2/M phase. **Conclusion:** RES has a role for attenuation of HCC through suppression of hepatocyte EMT. This could be via modulation of Akt/GSK3β/SNAIL1 pathway, induction of apoptosis and alleviation of oxidative stress.

Keywords: Resveratrol, hepatocellular carcinoma, epithelial-mesenchymal transition, Akt/GSK3β/SNAIL1 pathway, oxidative stress, apoptosis.

1.Assistant Professor of Biochemistry, Department of Biochemistry, Faculty of Pharmacy, Minia University, Minia 61519, Egypt .

2.Assistant Lecturer of Biochemistry, Department of Biochemistry, Faculty of Pharmacy, Deraya University, Minia, Egypt

3.Professor of Pharmacology and Experimental Oncology, Pharmacology and Experimental Oncology Unit, National Cancer Institute, Cairo University, Cairo 11796, Egypt

4.Lecturer of Pharmacology and Experimental Oncology, Pharmacology and Experimental Oncology Unit, National Cancer Institute, Cairo University, Cairo 11796, Egypt

1. BACKGROUND

Hepatocellular carcinoma (HCC) is a serious illness that poses a risk to both the health and survival of humans. It symbolizes dreadful scenarios in which there is uncontrollable cell proliferation, which leads to invasion of the surrounding tissues and eventually metastasis. Chemoprevention has received a lot of attention as a key tactic in reducing the present morbidity and mortality associated with this affliction, as a result of the limited therapeutic response and poor prognosis of liver cancer. The etiology of HCC may be influenced by several environmental, genetic and epigenetic variables (1). One of the most significant

Eur. Chem. Bull. **2023**,*12(Special issue 8), 7788-7803*

7788

Resveratrol slows down epithelial-mesenchymal transition in hepatocellular carcinoma via modulation of Akt/GSK3β/SNAIL1 signaling pathway

Section A -Research paper

environmental factors that contribute to liver cancer is diethylnitrosamine (DEN). DEN is used as lubricant additive and stabilizer for industry materials. Direct exposure to DEN is followed by metabolism into reactive intermediates. This is the primary cause of DEN-induced DNA damage that not only induces mutations in the liver cells, but also enhances postnecrotic hepatocellular proliferation. Because of its relatively simple metabolic pathway and potent carcinogenic activity, DEN is a well-known model for HCC to study cancer biology and therapeutic efficacy of many drugs (2).

The dynamic process known as epithelial-mesenchymal transition (EMT) transforms immobile, polarized epithelial cells into mobile, migratory mesenchymal cells, acting as a key mechanism in the development of tumor invasion, metastasis and recurrence. It entails a number of steps, including the separation of intercellular connections between epithelial cells, the loss of epithelial biosignatures, and the acquisition of mesenchymal cell phenotypic characteristics. Transforming growth factor-β1 (TGF-β1) is regarded as the primary inductor of EMT which takes place through different signaling pathways (3). The Akt/Glycogen synthase kinase-3 beta (Akt/GSK3β) pathway is one of the signaling pathways that has been discovered to play a central role in the regulation of EMT during HCC. The initiation of Akt in this pathway deactivates GSK3β, which subsequently dephosphorylates SNAIL1 and facilitates its nucleation, eventually inducing EMT. Further evidence that SNAIL1 plays a role during EMT comes from its association with lower expression levels of E-cadherin and its replacement by N-cadherin. In view of this background, understanding the mechanism of EMT, disrupting TGF-β1 production, blocking the Akt/GSK3β pathway, inhibiting oxidative stress and/or modulating apoptosis in hepatocytes will offer a potential strategy for management of HCC, bringing hope to millions of HCC patients worldwide.

Recent research has focused on the use of dietary polyphenols as a preventative and curative remedy for a variety of illnesses, including liver cancer. They are natural multi-targeting, less expensive, and present in natural foods with little to no side effects. One such polyphenol is resveratrol (RES), which is present in large quantities in grapes and peanuts. It has been noted that, RES has antioxidant, anti-inflammatory, anti-tumor, and anti-proliferative impacts against various diseases (4, 5). Accordingly, the current study was conducted with the following objectives; (1) to assess the possible anti-cancer action of RES *in vivo* in DEN/CCl4-induced hepatocarcinogenesis and the *in vitro* anti-proliferative effect in human hepatoma (HepG2) cell line, and (2) to gain knowledge about the potential of RES to provide mechanism-based protection against HCC through suppression of EMT via modulation of Akt/GSK3β/SNAIL1 signaling pathway and induction of apoptosis.

2. METHODS

2.1. Materials

DEN and CCl4 were purchased from Sigma Chemical Co. (St. Louis, MO, USA). DEN was dissolved in normal saline, while CCl4 was utilized as a 1:1 dilution in corn oil. RES powder was ordered from Schnelldorf, Germany. RES was freshly dissolved in a 0.5% carboxymethyl cellulose aqueous solution. The highest analytical grade was chosen for all additional compounds.

2.2. Animals & Experimental Design:

In order to accomplish the study's main objective, a total of 50 adult male Wistar albino rats, weighed 180–200 g, were acquired from Nahda University (NUB) animals house, Beni-Suef, Egypt. Animals were divided into five groups, ten rats each, as follows: Group-1 (normal control group): rats received the vehicles only including normal saline by gavage daily for 15 weeks, a single intraperitoneal (*i.p.*) injection of normal saline, and subcutaneous (*s.c.*) injection of corn oil twice a week for 15 weeks (6); Group-2 (RES group): RES dissolved in normal saline was administered by gavage (100 mg/kg/day) daily for 15 weeks (7); Group-3 (DEN/CCl4 group): A single *i.p.* injection of DEN, dissolved in normal saline, was administered (200 mg/kg) (8, 9), and two weeks later, rats received *s.c.* injections of 1:1 (v/v) CCl4 in corn oil (3 ml/kg/week) twice a week until the end of the 15 weeks (10); Group-4 (pre-HCC treatment group): rats received RES by gavage (100 mg/kg/day) daily, starting a week before receiving DEN/CCl4 same as group 3, and RES administration was continued until the end of the 15 weeks; Group-

*Eur. Chem. Bull. **2023**,12(Special issue 8), 7788-7803*

7789

Resveratrol slows down epithelial-mesenchymal transition in hepatocellular carcinoma via modulation of Akt/GSK3β/SNAIL1 signaling pathway

Section A -Research paper

5 (post-HCC treatment group): received a single *i.p.* injection of DEN (200 mg/kg), and two weeks later, rats received *s.c.* injections of 1:1 (v/v) CCl_4 in corn oil (3 ml/kg/week) twice a week in addition to RES by gavage (100 mg/kg/day) daily until the end of the 15 weeks. Animals were starved overnight after receiving the final dosages of the treatment protocol, and then slaughtered under ether anesthesia (2%). By decapitating the subject, blood samples were drawn from the neck veins, allowed to coagulate, and then centrifuged at 1500x g for 10 min to extract the serum. The serum was then put into sterile polypropylene tubes and stored at -80˚C for later examination. Liver tissue was swiftly removed, cleaned, dried, and divided into two halves. One half was stored in 10% formalin for histopathological examinations. The other half was homogenized in lysis buffer (20 mM Tris, 1 mM EDTA, 100 mM NaCl, protease inhibitors, and 0.5% Triton X-100 buffer). The tissue homogenate was centrifuged, and the resulting supernatant was stored as aliquots in Eppendorf tubes at -80˚C until use for western blotting and biochemical determinations. Biuret test results were used to calculate protein concentration (11).

2.3. *In vitro* cell culture and drug treatment

Human hepatic carcinoma (HepG2) cell line was purchased from the American Type Culture Collection (ATCC, Minisota, U.S.A.) and cultured in Dulbecco's Modified Eagle's medium (Thermo Fisher Scientific, Inc., Waltham, MA, USA) supplemented with 10% fetal bovine serum and 1% penicillin-streptomycin mixture for 24 h at 37°C in a humidified environment with 5% CO_2.

2.4. Cell viability assay

Cell viability was assessed using Sulforhodamine B (SRB) cytotoxicity assay, as previously described (12). HepG2 cells were seeded in 96-well culture plates at a density of 4×10^3 cells per well, and they were then cultivated in 200 µl fresh media for 24 h until they adhered. The cells were incubated with various RES concentrations for 48 h. The cells were then fixed with 10 µl cold trichloroacetic acid (10% final concentration) for 1 h at 4°C, washed with distilled water using an automated washer (Tecan, Germany), and stained with 50 µl 0.2 % SRB dissolved in 1 % acetic acid for 30 min in the dark at room temperature. The dye

was solubilized in 200 µl of 10 M tris base (pH 10.5), and the optical density was measured at 570 nm with an enzyme-linked immunosorbent assay (ELISA) microplate reader (Sunrise Tecan reader, Germany). The optimum IC_{50} (half-maximum inhibitory concentration) value was determined.

2.5. Apoptosis and cell cycle analysis by flow cytometry

Annexin-V FITC/ Propidium Iodide (PI) double staining was performed to identify early apoptotic (annexin V positive, PI negative) and late apoptotic (annexin V positive, PI positive) cells, necrotic (annexin V negative, PI positive) and viable (annexin V negative, PI negative) using Annexin-V FITC kit, following the manufacturer's guidelines (Beckman Coulter Inc., Brea, CA, USA). In a nutshell, trypsin was used to extract the cells, which were then suspended in binding buffer after being washed three times with PBS. After that, the suspension was incubated with Annexin-V and PI for 15 min at room temperature. Using the flow cytometry system FACStar (Becton Dickinson), the fluorescence of cells was assessed (13).

2.6. Biochemical analysis

Using commercially available kits (Biodiagnostic, Egypt), serum was examined for the liver marker enzymes, serum alanine aminotransferase (ALT) and serum aspartate aminotransferase (AST) activity according to published techniques (14). The My BioSource Rat α-fetoprotein ELISA Kit was used according to the manufacturer's instructions in order to quantitatively measure the α-fetoprotein (AFP) level (15). A 10% homogenate of liver tissue was used to determine L-malondialdehyde (L-MDA) concentration (16), catalase (CAT) (17), superoxide dismutase (SOD) (18) and glutathione peroxidase (GSH-Px) activity (19).

2.7. Western blotting analysis for hepatic TGF-β1, SNAIL1 and E-cadherin expression

After boiling samples containing an identical amount of proteins (50 µg) with loading buffer solution containing 2-mercaptoethanol at 95°C for 5 min, the samples were loaded onto 12% sodium dodecyl sulfate- polyacrylamide gel electrophoresis (SDS-PAGE) gel, and then transferred onto polyvinylideneflouride (PVDF) membrane. The membranes were incubated with

*Eur. Chem. Bull. **2023**,12(Special issue 8), 7788-7803*

7790

primary antibodies from rabbits for TGF-β1, SNAIL1, E-cadherin, and β-actin (1:1000; Santa Cruz Biotechnology, Santa Cruz, CA) overnight at 4°C after being blocked for 1 h in 5% (w/v) non-fat milk in tris-buffered saline (TBS-T) blocking solution. The membranes were then washed and treated with HRP- conjugated polyclonal goat anti-rabbit secondary antibodies for 1 h (1:5000; Cell Signaling Technology Inc., MA, USA). Protein bands were visualized using 5-bromo-4-chloro-3-indolyl phosphate (BCIP)/nitro-blue tetrazolium (NBT). The densitometry measurements were calculated using Image J Software. Densities of the bands were normalized to the corresponding β-actin band densities and calibrated as a fold-change value from the normal control.

2.8. Histopathological examination

Dehydrated liver tissue samples that had been phosphate buffered formalin-fixed were embedded in blocks of paraffin wax. Sections that were 4 μm thick were stained using hematoxylin-eosin (H&E) staining. The slides were anonymously coded and viewed at magnification X40 with the light microscope (Leika DMRBE, Germany) (20).

2.9. Immunohistochemical examination

For the immunohistochemical evaluations, sections (4 μm thick) were de-waxed in xylene for 30 min and re-hydrated in an alcohol bath solution. Antigen retrieval was carried out by treating the sections with sodium citrate buffer (pH. 6.0) for 15 min in microwave oven, and then rinsed with phosphate buffered saline (PBS). To inhibit endogenous peroxidase activity, sections were treated with 3% H_2O_2 at 37°C for 10 min. The slides were washed in PBS and then incubated for 60 min at room temperature with the primary antibodies for p-Akt and GSK3β from Santa Cruz Biotechnology, Inc. in Dallas, Texas (sc-16646-R and 22104-1-AP, respectively). The slides were then washed and treated for 30 min with secondary antibodies. The slides were counter stained with 3,3'-diaminobenzidine and hematoxylin solution. p-Akt or GSK3β expression was assessed based on the intensity and the percentage of positively stained cells. On a scale of 0 to 4, staining intensity was determined as follows: 0 (no staining), 1 (weakly positive staining), 2 (moderately positive staining), 3 (strong staining), and 4 (extremely strong staining). The percentage of cells was scored as (0%), 1 (10%-25%), 2 (26%-50%), 3 (51%-75%), and 4 (76%-100%) by the percentage of labelled cells (0-100%) multiplied by the percentage of labeled cells (0-100%) producing scores (21). A score that was higher than or equal to the mean was categorised as "high" immunostaining, whereas a score that was lower than or equal to the mean was categorised as "low" immunostaining.

2.10. Statistical analysis

Data were analyzed with one-way analysis of variance (ANOVA) and Tukey–Kramer post-analytical test using GraphPad® Prism V.5.0 software (GraphPad® Prism Inc, California, USA). Results were presented as Mean ± SEM. p-values < 0.05 were deemed evidence for statistical significance.

3. RESULTS
3.1. Effect of RES on hepatic injury indices

As shown in **Fig. 1**, in comparison to normal control group, serum ALT and AST levels in DEN/CCl$_4$ group were significantly higher ($p < 0.01$). However, compared to DEN/CCl$_4$ group, there was a significantly lower serum level of these biochemical markers in pre-HCC and post-HCC treatment groups. Noticeably, RES group showed insignificant changes in the serum enzyme levels compared to normal control group, implying that RES-dependent effects are selective or restricted to HCC-rats. Additionally, compared to post-HCC treatment group, pre-HCC treatment group's serum levels of ALT and AST were more significantly decreased.

Similarly, the serum level of AFP showed a significant elevation in DEN/CCl$_4$-rats ($p < 0.01$) when compared to normal controls. Upon subsequent treatment with RES, a significant reduction in the serum levels of this parameter was achieved. Furthermore, the effect of RES was more evident in pre-HCC treatment group than in post-HCC treatment group.
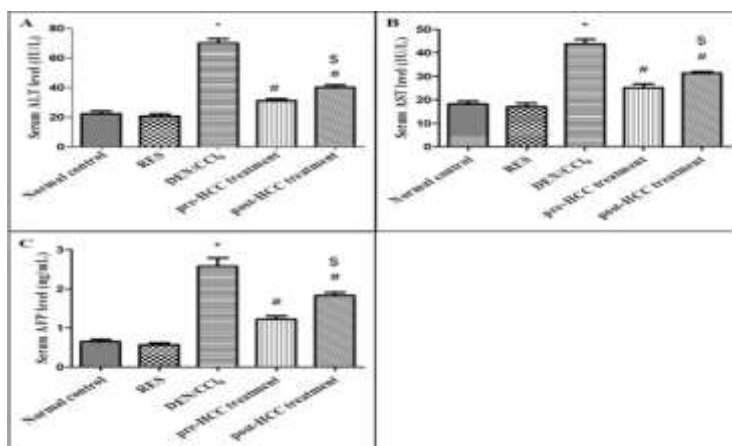
Fig. 1. Effect of RES on serum ALT (A), AST (B) and AFP (C) levels, in a model of hepatocellular carcinoma in rats. Data are expressed as Mean ± SEM (n = 6 rats). *, [#] and [$] indicate significant change from normal control, DEN/CCl4 and pre-HCC treatment groups, respectively, at $p < 0.05$ using One-way ANOVA followed by Tukey–Kramer as a post ANOVA test. RES: Resveratrol, DEN: Diethylnitrosamine, CCl4: Carbon tetrachloride.

3.2. Effect of RES on hepatic oxidative stress parameters

In comparison to normal control group, DEN/CCl4 group exhibited a substantial rise in liver MDA concentration ($p < 0.001$, **Fig. 2A**), and a substantial drop in SOD, CAT, and GSH-Px activities ($p < 0.01$, **Fig. 2B, C, D**). It's intriguing to note that administering RES to rats with HCC reversed the effects of DEN/CCl4 on the above-mentioned parameters. Between RES group and normal control group, there were no appreciable differences. Besides, RES in pre-HCC treatment group produced obvious impacts on the concentration of MDA as well as the activities of SOD, CAT and GSH-Px in the hepatic tissues compared to that produced by RES in post-HCC treatment group.
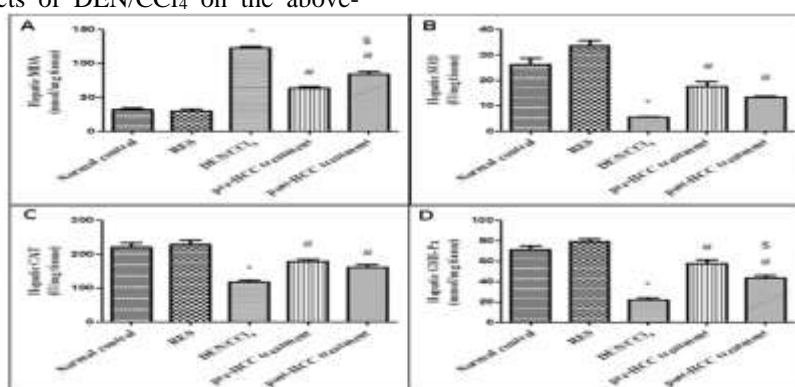
Fig. 2. Effect of RES on hepatic MDA (A), hepatic SOD (B), hepatic CAT (C) and hepatic GSH-Px (D) levels, in a model of hepatocellular carcinoma in rats. Data are expressed as Mean ± SEM (n = 6 rats). *, [#] and [$] indicate significant change from normal control, DEN/CCl4 and pre-HCC treatment groups, respectively, at $p < 0.05$ using One-way ANOVA followed by Tukey–Kramer as a post ANOVA test. RES: Resveratrol, DEN: Diethylnitrosamine, CCl4: Carbon tetrachloride.

3.3. Effect of RES on hepatic TGF-β1, SNAIL1 and E-cadherin expression

Western blotting demonstrated a considerable up-regulation of TGF-β1 and SNAIL1

coupled with a down-regulation of E-cadherin expression levels in the liver homogenates collected from DEN/CCl$_4$ rats compared to the normal controls after normalizing the intensities of bands to the β-actin loading control. On the contrary, DEN/CCl$_4$ group rats co-administered with RES displayed a clearly decreased ($p < 0.01$) level of

TGF-β1 and SNAIL1 hepatic protein expression as well as a clearly increased level of E-cadherin expression in comparison to the expression levels in DEN/CCl$_4$ group. Additionally, delivery of RES prior to DEN/CCl$_4$ exerted greater effects on the expression levels than did RES post-treatment (**Fig. 3A–D**).
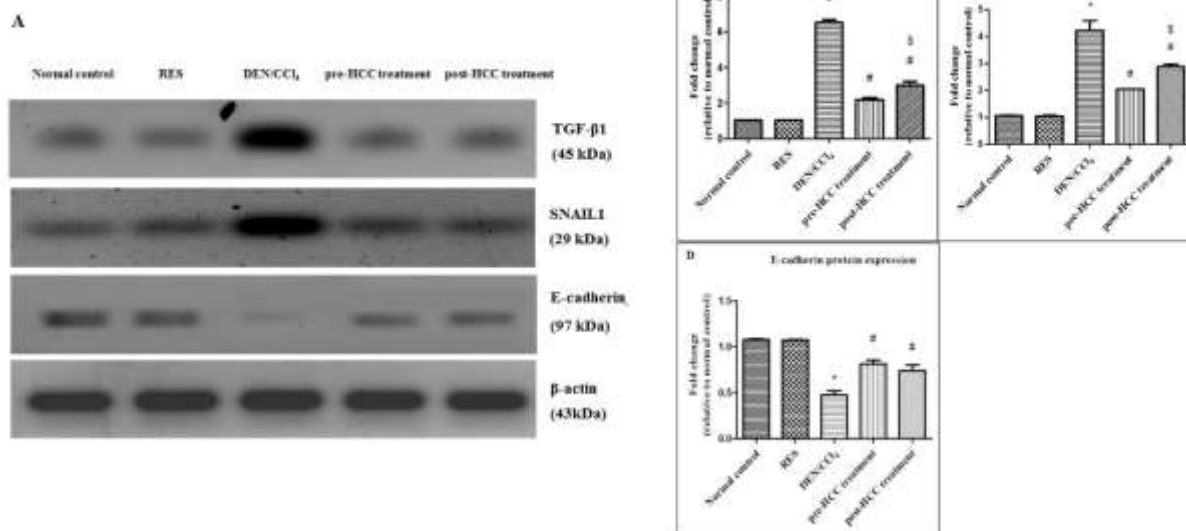
Fig. 3. Effect of RES on TGF-β1, SNAIL1 and E-cadherin protein expression in a model of hepatocellular carcinoma in rats. Data are reported as: (A) representative electrophoretic analysis of Western blotting products. β-actin was used as an internal control. (B), (C), and (D) graphs represent relative densities of TGF-β1, SNAIL1 and E-cadherin protein bands, respectively. RES: Resveratrol, DEN: Diethylnitrosamine, CCl$_4$: Carbon tetrachloride.

3.4. Effect of RES on hepatic histopathological changes

Paraffin-embedded sections from different groups were used to evaluate and compare histopathological alterations after different treatments. Study of the hepatic sections from rats in normal control (A) and RES (B) groups revealed no histopathological alterations and approximately normal hepatic architecture, indicating the non-toxic nature of RES (**Fig. 4A, B**). However, the study of hepatic sections obtained from rats subjected to DEN/CCl$_4$ treatment showed focal areas of hepatocytes in the parenchyma not well demarcated from the surrounding and characterized by an

abnormal growth pattern consistent with criteria of malignancy as hyperchromatic nuclei, polarity and pleomorphism. Thickening of the Glisson's capsule, inflammatory cells infiltration, fibroblastic cells proliferation, hepatocytes degeneration and dilatation of the portal vein were prominent (**Fig. 4C–F**). Group of rats pre-treated with RES showed a moderate fatty change in the hepatocytes and focal inflammatory cells infiltration in other areas of the parenchyma (**Fig. 4G**). Group of rats post-treated with RES showed focal inflammatory cells infiltration and fibroblastic cells proliferation underneath the thick Glisson's capsule surrounding the bile ducts and dilated portal vein (**Fig. 4H**)
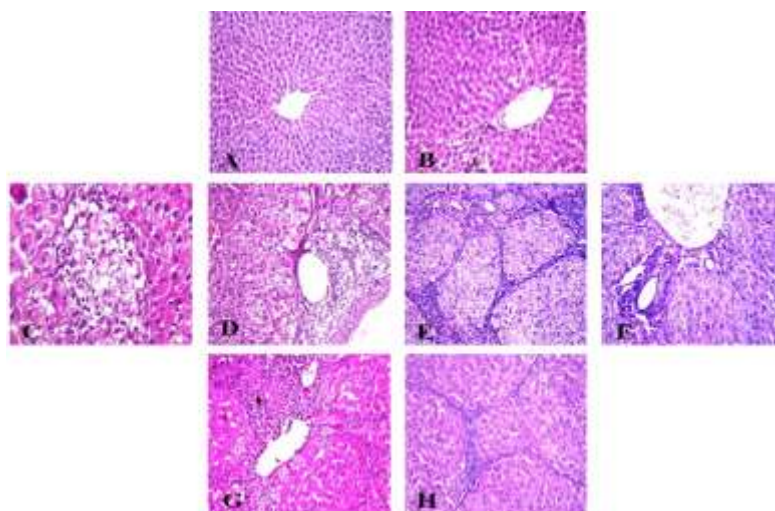
Fig. 4. Light microscopic examination of hepatic sections of: **(A)** normal control and **(B)** RES group showing no histopathological alterations; **(C)** DEN/CCl$_4$ group showing focal areas of hepatocytes in the parenchyma not well demarcated from the surrounding, and **(D)** characterized by an abnormal growth pattern consistent with the criteria of malignancy, associated with **(E)** thickening of the Glisson's capsule and **(F)** inflammatory cells infiltration as well as fibroblastic cells proliferation surrounding the bile ducts and dilated portal vein; **(G)** pre-HCC treatment group showing moderate fatty change in the hepatocytes with focal inflammatory cells infiltration in other areas of the parenchyma; **(H)** post-HCC treatment group showing fine fibroblastic cells proliferation in between the hepatocytes associated with inflammatory cells infiltration in the portal area (H&E, x40).

3.5. Effect of RES on hepatic immunohistochemical changes

p-Akt and GSK3β expression levels did not differ significantly between the normal control and RES groups. However, we found a statistically significant difference between normal control group and DEN/CCl$_4$ group. p-Akt expression was +4 in DEN/CCl$_4$ group (**Fig. 5**). In comparison to DEN/CCl$_4$ group, pre-HCC treatment and post-HCC treatment groups displayed a decrease in p-Akt expression. More reduction was observed in p-Akt expression level in pre-HCC treatment group (+2) than in post-HCC group (+3) (**Table 1**).

On the other hand, GSK3β expression was +1 in DEN/CCl$_4$ group (**Fig. 6**). There was a significant increase in GSK3β expression level in pre-HCC treatment and post-HCC treatment groups when compared to DEN/CCl$_4$ group. Notably, the elevating influence of RES on the expression level of GSK3β was more pronounced in pre-HCC treatment group (+3) than that caused by RES in post-HCC treatment group (+2) (**Table 2**).
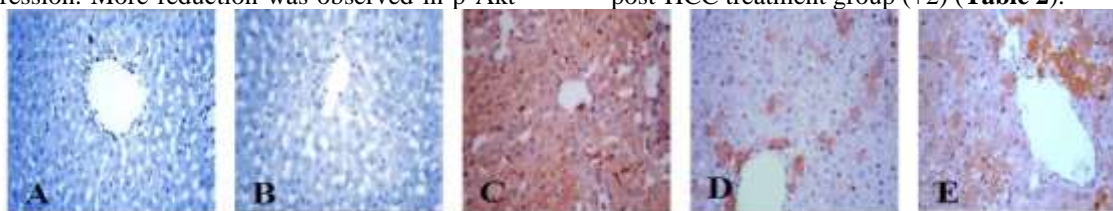

Fig. 5. Immunohistochemical staining for p-Akt expression of: (A) normal control and (B) RES groups showing no expression; (C) DEN/CCl$_4$ group showing very strong expression; (D) pre-HCC treatment group showing moderately positive staining and (E) post-HCC treatment group showing strong positive staining.
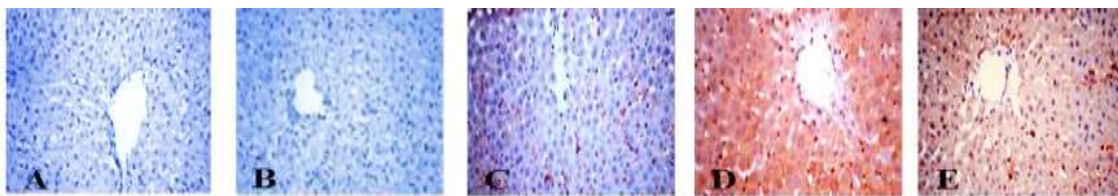
Fig. 6. Immunohistochemical staining for GSK3β expression of: (A) normal control and (B) RES groups showing no expression; (C) DEN/CCl₄ group showing weakly positive staining; (D) pre-HCC treatment group showing strong positive staining and (E) post-HCC treatment group showing moderately positive staining.

Table 1. Scoring of the immunohistochemical changes of p-Akt associated with DEN/CCl₄ administration and its alteration by various treatments.

Groups	No. of immunostained cells per field X40					Score
Normal control	0	1	0	3	0	0
RES	0	0	2	1	2	0
DEN/CCl₄	78	95	83	98	89	4
pre-HCC treatment	18	14	17	22	19	2
post-HCC treatment	40	22	42	33	27	3

Score level **0** was considered no changes. Scores 1, 2, 3 and 4 are weakly positive, moderately positive, strong, very strong levels, revealing less than 25, 25, 50, and 75% immunohistochemical alterations of total fields examined, respectively. Score represents values obtained from tissue sections of 5 animals of each group, 5 fields/section. DEN: Diethylnitrosamine, CCl₄: Carbon tetrachloride, RES: Resveratrol.

Table 2. Scoring of the immunohistochemical changes of GSK3β associated with DEN/CCl₄ administration and its alteration by various treatments.

Groups	No. of immunostained cells per field X40					Score
Normal control	0	0	0	1	0	0
RES	0	0	1	1	0	0
DEN/CCl₄	8	13	11	15	7	1
pre-HCC treatment	60	69	71	66	73	3
post-HCC treatment	28	37	32	39	36	2

Score level **0** was considered no changes. Scores 1, 2, 3 and 4 are weakly positive, moderately positive, strong, very strong levels, revealing less than 25, 25, 50, and 75% immunohistochemical alterations of total fields examined, respectively. Score represents values obtained from tissue sections of 5 animals of each group, 5 fields/section. DEN: Diethylnitrosamine, CCl₄: Carbon tetrachloride, RES: Resveratrol.

3.6. Effect of RES on cell viability in HepG2 cells

The SRB test was used to assess the cytotoxic effect of RES on the viability of HepG2 cells. RES greatly reduced cell proliferation in a concentration-dependent (0-100 μM) manner **(Fig. 7)**. The IC$_{50}$ value was calculated to be (15.5 ± 0.2 μM) for HepG2 cells. The survival of cells was expressed as a percentage relative to that of the control cells. These findings revealed that, RES suppressed HepG2 cell proliferation to a larger extent.
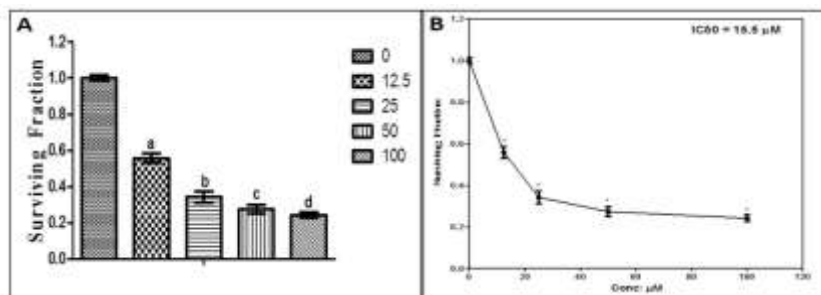
Fig. 7. Effect of RES towards HepG2 cells as determined by the SRB assay. (A) Cells were treated with specified concentrations of RES (0, 12.5, 25, 50 and 100 µM) for indicated time (24, 48, 72 h). The values for each RES concentration tested represent the mean ± SD from nine replicate wells and are representative of three separate experiments. a, b, c, and d indicate significant changes of corresponding group from control untreated cells (0 µM RES) at $p < 0.05$. (B) Calculating IC_{50} value for HepG2 cells.

3.7. Effect of RES on apoptosis in HepG2 cells

To detect the capacity of RES to trigger apoptosis, annexin V-FITC/PI dual staining assay was performed on both early and late apoptosis percentages in HepG2 cells. As demonstrated in **Fig. 8**, our results showed that the proportion of early apoptotic (annexin V+/PI-) cells was significantly increased from 0.34 ± 0.01% (untreated cells) to 26.1 ± 0.36% (treated cells). Also, the percentages of late apoptotic (annexin V+/PI+) cells was significantly increased from 0.31 ± 0.01% (untreated cells) to 60.6 ± 0.79% (treated cells). The percentage of total apoptotic cells was significantly increased from 0.47 ± 0.01% (untreated cells) to 49.7 ± 0.28% (treated cells) (**Fig. 9 and Table 3**).
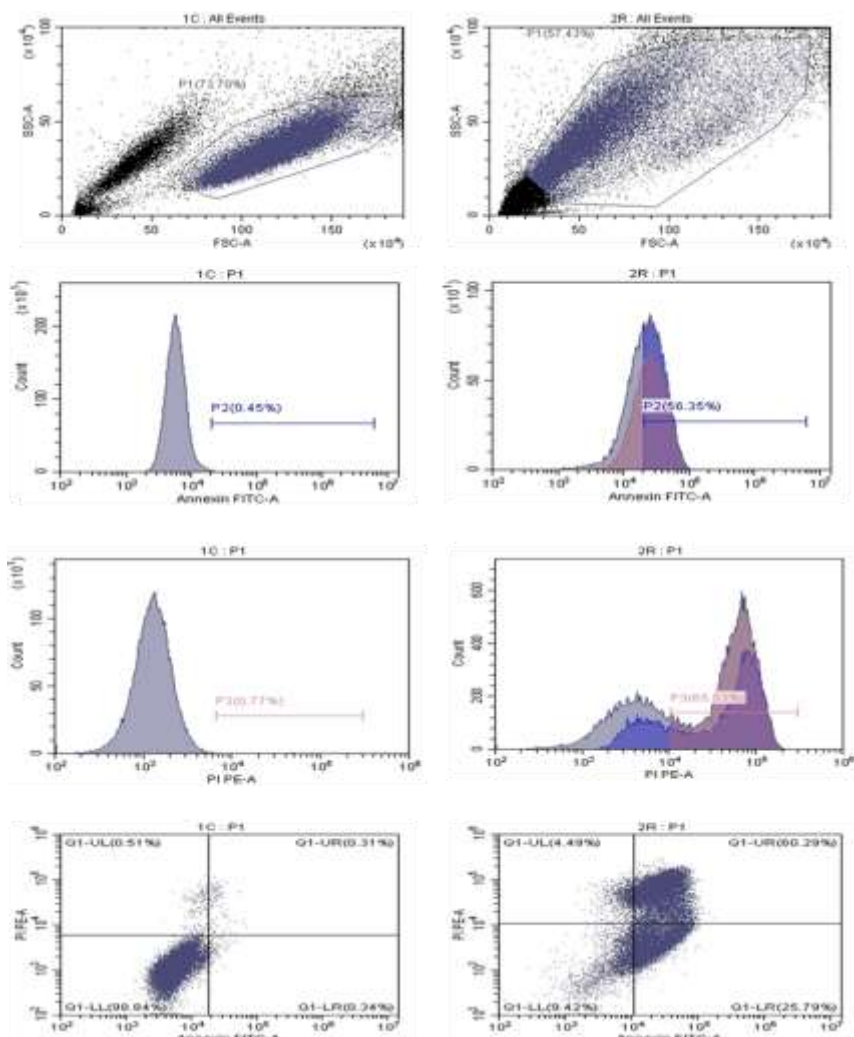
Fig. 8. Representative flowcytometric dot plots for Annexin V staining. (A) represents untreated HepG2 cells, while (B) represents treated HepG2 cells with RES for 48 h. X-axis represents FITC-conjugated Annexin V, and Y-axis represents PE-conjugated PI. Squares Q1-UL, Q1-UR, Q1-LL and Q1-LR indicate, necrosis, late apoptosis, viable and early apoptosis, respectively.
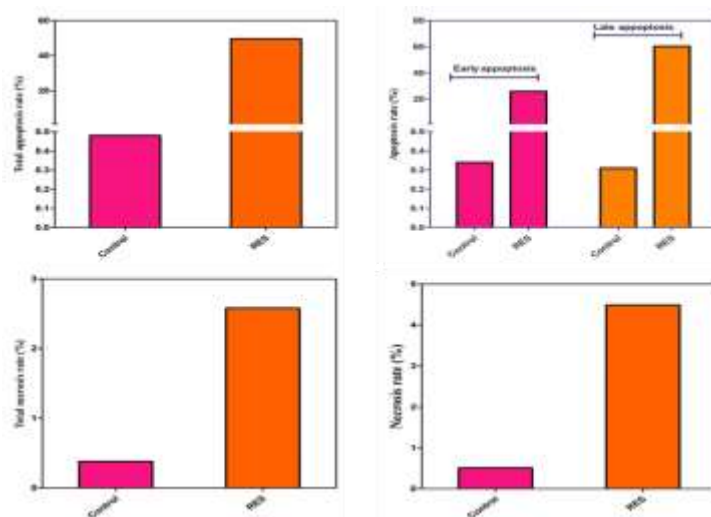
Fig. 9. Apoptotic cells before and after the treatment with RES for 24 h. Data are expressed as Mean ± SD of three separate experiments.

Table 3. Cell apoptosis before and after RES treatment for 24 h

Cells	Total apoptosis	Early apoptosis	Late apoptosis	Necrosis
HepG2/ Untreated	0.45 ± 0.01	0.34 ± 0.01	0.31 ± 0.01	0.37 ± 0.01
HepG2/ treated	*56.35 ± 0.28	*25.7 ± 0.36	*60.2 ± 0.79	*2.65 ± 0.04

Data are expressed as Mean ± SD of three separate experiments. * indicates significant change from control untreated cells, at $p < 0.05$ using One-way ANOVA followed by Tukey–Kramer as a post ANOVA test.

3.8. Effect of RES on cell cycle analysis in HepG2 cells

As the changes in cell cycle kinetics often precede induction of apoptosis, we investigated the cell cycle changes after the treatment with the IC_{50} of the drug for 24 h in HepG2 cells, as shown in **Fig. 10**. In agreement with the annexin V results, we found a significant decrease in % G0-G1 peak from 98.29 ± 0.17 (untreated cells) to 56.4 ± 0.32 (treated cells). Then, the cell proportion at the S phase increased from 0.91 ± 0.01 to 41.6 ± 0.25 when compared to untreated cells. Also, there was increase in the %G2-M phase from 0.31 ± 0.01 (untreated cells) to 0.62 ± 0.01 (treated cells) (**Fig. 11 and Table 4**).
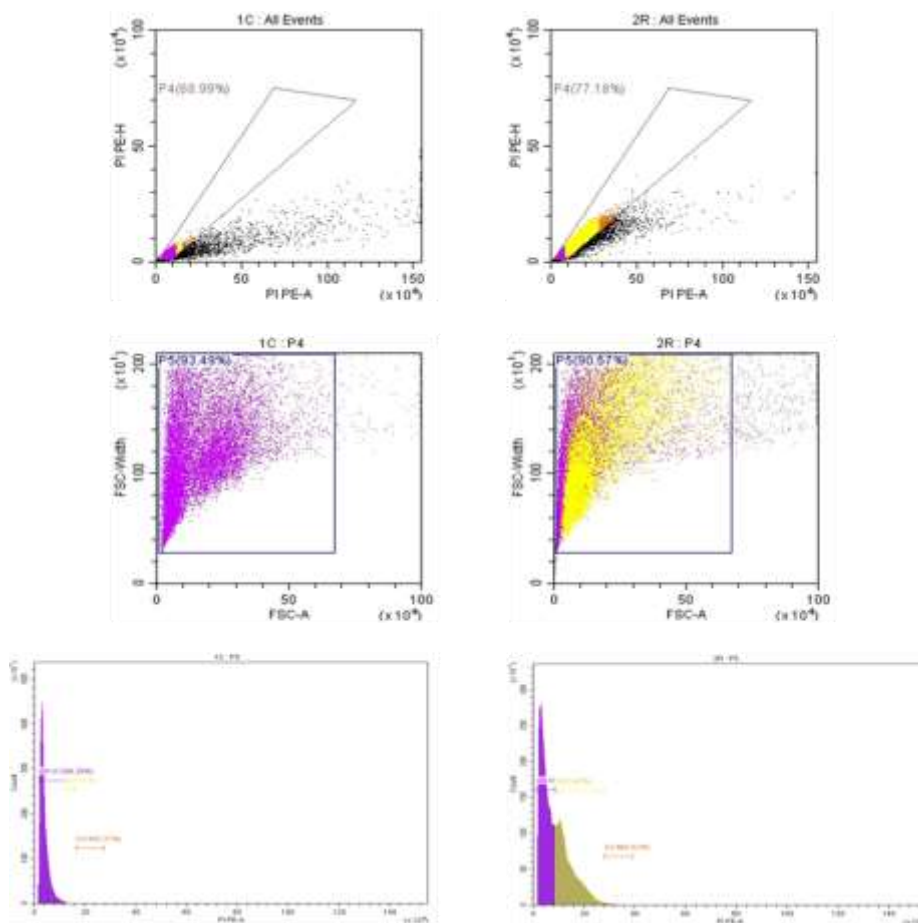
Fig. 10. Representative histograms of the cell cycle phase distribution after PI staining for untreated and treated HepG2 cancer cells with the IC_{50} of the drug for 24 h determined by flow cytometric analysis.
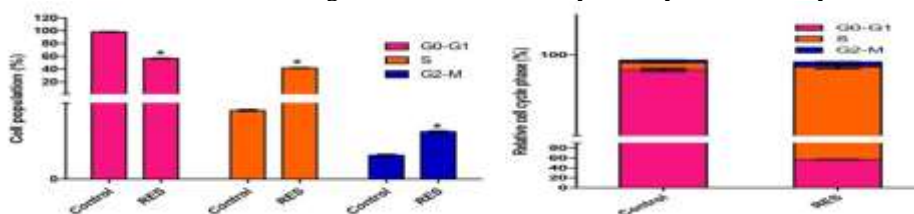

Fig. 11. Distribution of cell cycle phases of untreated and treated cells with IC_{50} of the drug for 24 h. Data are expressed as Mean ± SD of three separate experiments.

Table 4. Percentage of the cell cycle phases for untreated and treated cells with the IC_{50} of the drug for 24 h.

Cells	% G0 – G1	% S	% G2 - M
HepG2/untreated	98.2 ± 0.17	0.91 ± 0.01	0.31 ± 0.01
HepG2/ treated	*56.40 ± 0.32	*41.65 ± 0.25	*0.62 ± 0.01

Data are expressed as Mean ± SD of three separate experiments. * indicates significant change from control untreated cells at $p < 0.05$ using One-way ANOVA followed by Tukey–Kramer as a post ANOVA test.

4. DISCUSSION

HCC is an aggressive dreadful malignancy that places a huge strain on the health care systems and the drug regulatory agencies as well. Therefore, the efforts to inspect new strategies for hepatoprotection and treatment of HCC are urgently needed.

Under physiological conditions, the epithelial hepatocytes are mitotically inactive, highly differentiated and tend to express many epithelial markers like E-cadherin. But in case of pathophysiological conditions such as wound healing and carcinoma progression, the expression of E-cadherin is down-regulated, and mesenchymal markers start to be expressed and induce an EMT state which eventually leads to invasion and metastasis, poor survival and increased risk of cancer recurrence.

Chemically induced liver carcinogenesis, particularly that triggered by the environmental carcinogen DEN, has been recognized as one of the best-employed experimental models of carcinogenesis, in the search of potential natural or synthetic compounds for cancer management. DEN is an *N*-nitroso alkylating agent, known to induce DNA alkylation leading to mutations paving the way to malignant transformation. Additionally, the promotion with CCl_4 is the leading to centrilobular necrosis and cellular infiltration of the liver, thereby creating a microenvironment that more imitates the clinical setting in which human HCC arises (22). After their use, a string of pre-neoplastic foci, neoplastic nodules followed by HCC nodules of various sizes have been observed. These markers represent surrogate end-point biomarkers in rat liver carcinogenesis model.

Metabolism of DEN in the liver by cytochrome P450 oxygenase system generates reactive oxygen species (ROS) that are assumed to be the catalyst for initiation of lipid peroxidation chain reaction with the formation of many hazardous products including MDA. These products can cause irretrievably covalent adducts with phospholipids leading to membrane disruption and with proteins impairing their functions. ROS and free radicals can also cause depletion of hepatic tissue antioxidant defense enzymes (i.e. catalase, superoxide dismutase and glutathione peroxidase) system. This in turn triggers mitochondrial malfunction and liver cell injury. Accordingly, our results showed that, DEN/CCl_4 caused a striking hepatic morphological abnormality manifested by histological examination. It also exhibited a remarkable elevation in the liver enzyme ALT and AST activities as well as serum AFP levels as previously reported (23). In addition, DEN/CCl_4 induced oxidative stress, which is evident in previous studies by the higher levels of MDA along with decreased CAT, SOD, GSH-Px activities in hepatic tissues.

As oxidative stress builds up, TGF-β1 expression and activation of hepatic stellate cells are eventually triggered. This promotes the trans-differentiation to myofibroblasts with subsequent excessive extracellular matrix production and reduced metabolism. Several lines of evidence have indicated that, TGF-β1 can induce the occurrence of EMT. It exerts its effect by inducing the SNAIL1 transcription factor which is implicated in the direct suppression of E-cadherin transcription, ultimately leads to EMT, hence HCC (24). In harmony with these findings, there was a marked increase in the protein expression levels of TGF-β1 and SNAIL1 with a concomitant decrease in the E-cadherin protein expression in livers of HCC rats.

A considerable attention has been paid to study the Akt/GSK3β signaling pathway since its important role in promoting EMT and metastasis. Blockade of Akt/GSK3β pathway could be a promising strategy, which aims at protecting hepatocytes from EMT, thus controlling HCC. This pathway is initiated by Akt activation that can phosphorylate various substrates, thus modulating their functions in cell survival, cell cycle progression and growth. The first of these is GSK3β, an upstream apoptotic regulator, resulting in its inactivation, thus inhibiting apoptosis.

In the ongoing study, we found that Akt expression was up-regulated, while GSK3β expression was down-regulated by DEN/CCl_4 combination in rats. We also observed that RES

caused significant improvement in hepatic injury indices. This action was referred to its membrane stabilizing activity leading to suppressing escape of the enzymes into the blood circulation. Diminishment in serum hepatic tumor marker AFP levels after RES administration is also indicative of its antineoplastic and anti-inflammatory effects as well. Administration of RES (either pre-treatment or post-treatment) also abrogated oxidative stress as evidenced by reducing the elevated hepatic levels of MDA, together with increasing the enzymatic antioxidant guard compared to HCC rats. The RES action might be attributed to the minimized production of free radicals, enhancement of the antioxidant status beyond its free radical scavenging property and decreased hepatic lipoperoxide formation depending on the phenolic moiety present in its structure (25, 26).

In addition, RES was noticed to reduce TGF-β1 and SNAIL1 proteins expression and also restored E-cadherin expression in the liver of HCC rats, thus preventing or at least slowing down the progression of the disease. Furthermore, our immunohistochemical results indicated that, the expression levels of Akt and GSK3β were down- and up-regulated, respectively, by RES administration. Consequently, these results suggest that RES could reverse EMT, possibly through modulating the Akt/GSK3β/SNAIL1 signaling pathway.

We also tracked how RES affected cellular proliferation and apoptosis during carcinogenic events to gain insight into the further mechanisms of RES action. The sensitivity of HCC cells of human or rodent origin to RES has been demonstrated in numerous experimental studies (27). Hence, HepG2 cell line is the *in vitro* model system used in the current investigation. Previous researches have illustrated that RES inhibits the proliferation of various types of tumor cells *in vivo* and *in vitro* (28). Consequently, it was discovered that RES dose-dependently decreased the viability of HepG2 cells and arrested HepG2 cells in the G2/M phase. Thus, amendment of cell cycle progression may be one of the anti-cancer mechanisms of RES. Apoptosis or programed cell death is a rigorous and definite anticancer protective mechanism utilized to kill and destroy unwanted cells as well as cells that have DNA damage which could not be repaired. Several reports have previously elucidated that, RES induces apoptosis in a variety of human cancer cell lines (29). In this work, RES induced apoptosis in HepG2 cell line through its delayed action on the cell cycle, which was supported by the *in vivo* outcomes including modulation of distress signals, restoration of the membrane integrity, suppression of DNA degradation, and enhancement of the detoxification systems (30).

5. CONCLUSION

RES has a promising health benefits against HCC relying on its modulatory action on Akt/GSK3β/SNAIL1 signaling pathway, repression of oxidative stress along with inhibition of cell proliferation and induction of cell death by apoptosis. Based on our results, RES-dependent effects are selective or preferential to HCC-bearing rats with no or minimal effects on normal (non-HCC) rats. Therefore, we recommend the use of RES in the management of HCC. However, much work is required to fully prove the applicability of RES administration to HCC patients.

LIST OF ABBREVIATIONS

HCC	Hepatocellular carcinoma	**AFP**	Alpha fetoprotein
RES	Resveratrol	**MDA**	Malondialdhyde
DEN	Diethyl nitrosamine	**SOD**	Superoxide dismutase
CCl₄	Carbon tetrachloride	**CAT**	Catalase
EMT	Epithelial-mesenchymal transition	**GSH-Px**	Glutathione peroxidase
ALT	Alanine aminotransferase	**TGF-β1**	Transforming growth factor-beta1
AST	Aspartate aminotransferase	**GSK-3β**	Glycogen synthesis kinase-3beta

DECLARATIONS

REFERENCES

1. Raju SK, Vinoth Kumar S, Rajkapoor B, Pravin N, Dharmasivam D. Chemopreventive effect of Indigofera linnaei extract against diethylnitrosamine induced hepatocarcinogenesis in rats. Journal of Applied Pharmaceutical Science. 2016;6:199-209.
2. Karabekir SC, Özgörgülü A. Possible protective effects of resveratrol in hepatocellular carcinoma. Iran J Basic Med Sci. 2020;23(1):71-8.
3. Thiery J, Sleeman J. Thiery JP, Sleeman JPComplex networks orchestrate epithelial-mesenchymal transitions. Nat Rev Mol Cell Biol 7: 131-142. Nature reviews Molecular cell biology. 2006;7:131-42.
4. Mileo AM, Miccadei S. Polyphenols as Modulator of Oxidative Stress in Cancer Disease: New Therapeutic Strategies. Oxidative Medicine and Cellular Longevity. 2016;2016:6475624.
5. Athar M, Back JH, Kopelovich L, Bickers DR, Kim AL. Multiple molecular targets of resveratrol: Anti-carcinogenic mechanisms. Archives of biochemistry and biophysics. 2009;486(2):95-102.
6. Pezzuto JM. Resveratrol as an inhibitor of carcinogenesis. Pharmaceutical Biology. 2008;46(7-8):443-573.
7. Varoni EM, Lo Faro AF, Sharifi-Rad J, Iriti M. Anticancer Molecular Mechanisms of Resveratrol. Frontiers in Nutrition. 2016;3.
8. Shahin YR, Elguindy NM, Abdel Bary A, Balbaa M. The protective mechanism of Nigella sativa against diethylnitrosamine-induced hepatocellular carcinoma through its antioxidant effect and EGFR/ERK1/2 signaling. Environmental Toxicology. 2018;33(8):885-98.
9. Chang C-C, Chang C-Y, Lin P-C, Huang JP, Chen K, Yen T-H, et al. Administration of low-dose resveratrol attenuated hepatic inflammation and lipid accumulation in high cholesterol-fructose diet-induced rat model of nonalcoholic fatty liver disease. Chinese Journal of Physiology. 2020;63:149.
10. Pezzuto J, Aggarwal B, Shishodia S. Resveratrol in Health and Disease2006. 233 p.
11. Fathy M, Nikaido T. In vivo attenuation of angiogenesis in hepatocellular carcinoma by Nigella sativa. Turkish journal of medical sciences. 2018;48(1):178-86.
12. Skehan P, Storeng R, Scudiero D, Monks A, McMahon J, Vistica D, et al. New colorimetric

Resveratrol slows down epithelial-mesenchymal transition in hepatocellular carcinoma via modulation of Akt/GSK3β/SNAIL1 signaling pathway

Section A -Research paper

cytotoxicity assay for anticancer-drug screening. J Natl Cancer Inst. 1990;82(13):1107-12.

13. Kerr JF, Wyllie AH, Currie AR. Apoptosis: a basic biological phenomenon with wide-ranging implications in tissue kinetics. Br J Cancer. 1972;26(4):239-57.

14. Reitman S, Frankel S. A colorimetric method for the determination of serum glutamic oxalacetic and glutamic pyruvic transaminases. American journal of clinical pathology. 1957;28(1):56-63.

15. Mizejewski GJ. Alpha-fetoprotein structure and function: relevance to isoforms, epitopes, and conformational variants. Exp Biol Med (Maywood). 2001;226(5):377-408.

16. Ohkawa H, Ohishi N, Yagi K. Assay for lipid peroxides in animal tissues by thiobarbituric acid reaction. Analytical biochemistry. 1979;95(2):351-8.

17. Aebi H. Catalase in vitro. Methods in enzymology. 1984;105:121-6.

18. Nishikimi M, Appaji Rao N, Yagi K. The occurrence of superoxide anion in the reaction of reduced phenazine methosulfate and molecular oxygen. Biochemical and Biophysical Research Communications. 1972;46(2):849-54.

19. Paglia DE, Valentine WN. Studies on the quantitative and qualitative characterization of erythrocyte glutathione peroxidase. The Journal of laboratory and clinical medicine. 1967;70(1):158-69.

20. Bancroft JD, Gamble M. Theory and practice of histological techniques: Elsevier Health Sciences; 2008.

21. Hu Y, Lin X, Zuo S, Luo R, Fang W. Elevated GSK3β expression predicts good prognosis in hepatocellular carcinoma. International journal of clinical and experimental pathology. 2018;11(5):2776-83.

22. Bishayee A, Dhir N. Resveratrol-mediated chemoprevention of diethylnitrosamine-initiated hepatocarcinogenesis: inhibition of cell proliferation and induction of apoptosis. Chemico-biological interactions. 2009;179(2-3):131-44.

23. Plaa GL. Detection and evaluation of chemically induced liver injury. Principles and methods of toxicology. 1982:407-40.

24. Kaufhold S, Bonavida B. Central role of Snail1 in the regulation of EMT and resistance in cancer: a target for therapeutic intervention. Journal of Experimental & Clinical Cancer Research. 2014;33(1):62.

25. Simão F, Matté A, Matté C, Soares FM, Wyse AT, Netto CA, et al. Resveratrol prevents oxidative stress and inhibition of Na(+)K(+)-ATPase activity induced by transient global cerebral ischemia in rats. J Nutr Biochem. 2011;22(10):921-8.

26. Kumar A, Kaundal RK, Iyer S, Sharma SS. Effects of resveratrol on nerve functions, oxidative stress and DNA fragmentation in experimental diabetic neuropathy. Life Sci. 2007;80(13):1236-44.

27. Aggarwal BB, Bhardwaj A, Aggarwal RS, Seeram NP, Shishodia S, Takada Y. Role of resveratrol in prevention and therapy of cancer: preclinical and clinical studies. Anticancer research. 2004;24(5A):2783-840.

28. Ferraz da Costa DC, Fialho E, Silva JL. Cancer chemoprevention by resveratrol: The p53 tumor suppressor protein as a promising molecular target. Molecules. 2017;22(6):1014.

29. Delmas D, Jannin B, Cherkaoui Malki M, Latruffe N. Inhibitory effect of resveratrol on the proliferation of human and rat hepatic derived cell lines. Oncol Rep. 2000;7(4):847-52.

30. Sun ZJ, Pan CE, Liu HS, Wang GJ. Anti-hepatoma activity of resveratrol in vitro. World J Gastroenterol. 2002;8(1):79-81.

*Eur. Chem. Bull. **2023**,12(Special issue 8), 7788-7803*

7803